npg

Severe hypoxia induces complete antifolate resistance in carcinoma cells due to cell cycle arrest

S Raz[1], D Sheban[1], N Gonen[1,2], M Stark[1], B Berman[1] and YG Assaraf*[,1]

Antifolates have a crucial role in the treatment of various cancers by inhibiting key enzymes in purine and thymidylate biosynthesis. However, the frequent emergence of inherent and acquired antifolate resistance in solid tumors calls for the development of novel therapeutic strategies to overcome this chemoresistance. The core of solid tumors is highly hypoxic due to poor blood circulation, and this hypoxia is considered to be a major contributor to drug resistance. However, the cytotoxic activity of antifolates under hypoxia is poorly characterized. Here we show that under severe hypoxia, gene expression of ubiquitously expressed key enzymes and transporters in folate metabolism and nucleoside homeostasis is downregulated. We further demonstrate that carcinoma cells become completely refractory, even at sub-millimolar concentrations, to all hydrophilic and lipophilic antifolates tested. Moreover, tumor cells retained sensitivity to the proteasome inhibitor bortezomib and the topoisomerase II inhibitor doxorubicin, which are independent of cell cycle. We provide evidence that this antifolate resistance, associated with repression of folate metabolism, is a result of the inability of antifolates to induce DNA damage under hypoxia, and is attributable to a hypoxia-induced cell cycle arrest, rather than a general anti-apoptotic mechanism. Our findings suggest that solid tumors harboring a hypoxic core of cell cycle-arrested cells may display antifolate resistance while retaining sensitivity to the chemotherapeutics bortezomib and doxorubicin. This study bears important implications for the molecular basis underlying antifolate resistance under hypoxia and its rational overcoming in solid tumors.
Cell Death and Disease (2014) 5, e1067; doi:10.1038/cddis.2014.39; published online 20 February 2014
Subject Category: Cancer

Antifolates are antineoplastic agents, which are extensively used to treat a spectrum of solid tumors and hematologic malignancies.[1] Folic acid antagonists, including aminopterin and methotrexate, were first introduced in the late 1940s and produced the first remissions in leukemia and the first cures of choriocarcinoma.[2] Antifolates exert their cytotoxic activity by inhibiting key enzymes in the folate metabolic pathway, thus disrupting nucleotide biosynthesis and DNA replication, leading to programmed cell death.[1] As antifolates are hydrophilic drugs, which cannot transverse the plasma membrane, they rely on specific influx systems for their cellular uptake and pharmacologic activity.[1] The main influx transporters for (anti)folates are the recently identified proton-coupled folate transporter (PCFT), expressed predominantly in the small intestine and in several solid tumors; and the ubiquitously expressed reduced folate carrier (RFC).[1] Until recently, RFC was considered to be the only (anti)folate influx transporter, and antifolate resistance phenomena were largely associated with impaired RFC transport activity.[1,3] Therefore, lipid-soluble antifolates were introduced to the

oncology clinic to overcome antifolate resistance associated with impaired antifolate transport.[1,3]

The extracellular pH of solid tumors is more acidic when compared with normal tissues.[4] As the transport Vmax of RFC is markedly reduced under acidic pH,[5] whereas PCFT displays optimal transport activity,[6] PCFT is considered to be the most efficient antifolate influx transporter in solid tumors.[6,7] Hence, recent efforts to overcome antifolate resistance focus on the design of antifolates with enhanced selectivity toward PCFT.[8,9]

Apart from the acidic pH, studies demonstrated a hypoxia gradient in solid tumors, with the most severe hypoxia prevailing in the tumor core.[10,11] Several hypoxia-induced drug-resistance mechanisms have been described such as reduced generation of free radicals, increased production of reducing agents, increased activity of DNA repair enzymes, cell cycle arrest and induction of anti-apoptosis.[12] However, the impact of hypoxia on antifolate cytotoxicity in tumor cells is poorly characterized. We show here that severe hypoxia leads to a marked suppression of genes in folate metabolism

and (anti)folate- and nucleoside transporters (NTs). We show that carcinoma cells display complete resistance to various hydrophilic and lipophilic antifolates under severe hypoxic conditions due to lack of DNA damage and cell cycle arrest. Remarkably however, under severe hypoxia, carcinoma cells retained sensitivity to the proteasome inhibitor bortezomib and the topoisomerase II inhibitor doxorubicin, which are independent of cell cycle progression. These novel findings have important ramifications for the rational overcoming of antifolate resistance in solid tumors.

Results

Severe hypoxic conditions induce downregulation of folate metabolism genes. To explore the impact of hypoxia on tumor cell sensitivity to antifolates, we induced severe hypoxic conditions by either growing cells in a hypoxic chamber ($\leq 0.1\%$ O_2) or in the presence of dimethyloxallyl-glycine (DMOG), an established hypoxia-mimetic agent that stabilizes hypoxia-inducible factor 1-alpha (HIF-1α) by blocking its degradation via inhibition of prolyl hydroxylases.[13]

The pharmacological activity of antifolates relies on their net cellular accumulation, as determined by the intricate interplay between their influx and efflux as well as their intracellular retention via polyglutamylation catalyzed by folylpolyglutamate synthetase (FPGS).[1] Uptake proceeds predominantly via RFC and PCFT, whereas the main (anti)folate efflux transporters are the multidrug resistance protein1 (MRP1/ABCC1) and breast cancer resistance protein (BCRP/ABCG2).[1,14] Another determinant of antifolate cytotoxicity is the expression of their target enzymes: dihydrofolate reductase (DHFR), thymidylate synthase (TS) and glycinamide ribonucleotide transformylase (GARTF).[7] To determine the impact of hypoxia on gene expression by real-time PCR, HeLa cells were exposed to 0.5 mM DMOG for 18 h or to severe hypoxia for 24 h. To verify that severe hypoxic conditions were

actually achieved, we confirmed the up-regulation of the well established HIF-1α target genes,[12] vascular endothelial growth factor (VEGF) and glucose transporter 1 (Glut1) (Figure 1a). Moreover, we evaluated the expression of the key pyrimidine biosynthetic trifunctional enzyme carbamoyl-phosphate synthetase-2 aspartate transcarbamylase-dihydroorotase (CAD, Figure 1c), which was shown to be directly downregulated by HIF-1α.[15] We then evaluated the expression of the folate metabolism-related genes detailed above. As depicted in Figure 1b, all genes were significantly downregulated under both treatments, including the two main antifolate transporters, RFC and PCFT, with a decrease of up to 80% in gene expression levels, whereas MRP1 levels remained unchanged.

Three routes exist for the maintenance of proper intracellular nucleotide pools: a) de novo biosynthesis, which requires folate cofactors and is restricted to selected cell types; b) the salvage pathway, which utilizes intermediates from the degradation pathway of nucleotides; and c) influx of nucleosides from the extracellular milieu. Two families of NTs have been characterized: equilibrative nucleoside transporters (ENTs) 1–3, which mediate passive nucleoside uptake, and concentrative nucleoside transporters (CNTs) 1–3, which mediate the Na$^+$-coupled unidirectional influx of nucleosides.[16] As our results indicate suppression of genes in nucleotide biosynthesis under hypoxic conditions and as ENT1 and ENT2 were previously shown to be downregulated under hypoxia,[17,18] we assessed NTs gene expression. Following an initial screen, which verified that HeLa cells express ENT1–3 and CNT3, but not CNT1,2, we determined NTs gene expression under severe hypoxic conditions using real-time PCR. Under severe hypoxia, all of these NTs were significantly downregulated, with the exception of ENT3 (Figure 1c), whereas under DMOG treatment, a moderate decrease in the expression of ENT1–3 was observed, while CNT3 was reduced by over 80% (Figure 1c).
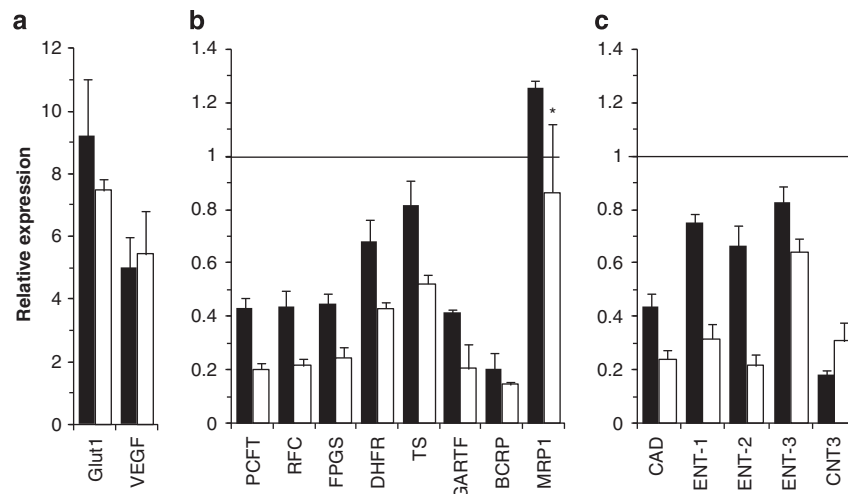
Figure 1 Genes in the folate metabolic pathway and nucleoside homeostasis are downregulated under severe hypoxic conditions. HeLa cells were exposed to either severe hypoxia ($\leq 0.1\%$ O_2) for 24 h (white) or 0.5 mM DMOG for 18 h (black), after which total RNA was extracted and real-time PCR analysis was performed to determine alterations in gene expression levels. (a) Established HIF-1α-responsive genes, (b) folate metabolism genes, and (c) nucleoside homeostasis genes. Relative gene expression shown is the ratio of treated cells to their untreated counterparts, normalized to β-glucuronidase (Gus-B). Results are the means of at least three independent experiments performed in triplicates $\pm$ S.D. $P \leq 0.008$ and $P \leq 0.03$ for hypoxia and DMOG, respectively, except for MRP-1 under hypoxia, denoted by an asterisk

Carcinoma cell lines exhibit a dramatic antifolate resistance under severe hypoxic conditions. The expression of *RFC* and *PCFT* was markedly decreased under severe hypoxic conditions, which should render the cells more resistant to hydrophilic antifolates that rely on these transporters for their cellular uptake. In contrast, when the target enzymes DHFR and TS are downregulated, cells become more sensitive to antifolates, particularly to lipophilic antifolates that do not depend on carrier-mediated transport but rather on simple diffusion.[3] Therefore, the cytotoxic activity of hydrophilic antifolates was compared with that of lipophilic antifolates and non-antifolate anticancer drugs following 72 h incubation of HeLa cells with increasing drug concentrations in the presence of 0.5 mM DMOG. Bortezomib

(BTZ), an established proteasome inhibitor, which was shown to retain its cytotoxicity under hypoxia,[19] was used as a control. In the presence of DMOG, HeLa cells were completely refractory to hydrophilic antifolates, including pemetrexed (PMX/MTA/Alimta, Figure 2a) and raltitrexed (Tomudex/ ZD1694, Figure 2b), but also to lipophilic antifolates, such as trimetrexate (TMQ/Neutrexin, Figure 2c) and piritrexim (PTX, Figure 2d), even at sub-millimolar concentrations. In fact, HeLa cells were completely refractory to every antifolate tested under DMOG treatment (i.e., plevitrexed, PT-523 and AG337, Supplementary Figure S1). In contrast, in the presence of DMOG, HeLa cells retained sensitivity to the non-antifolate chemotherapeutics doxorubicin (Figure 2e) and BTZ (Figure 2f).
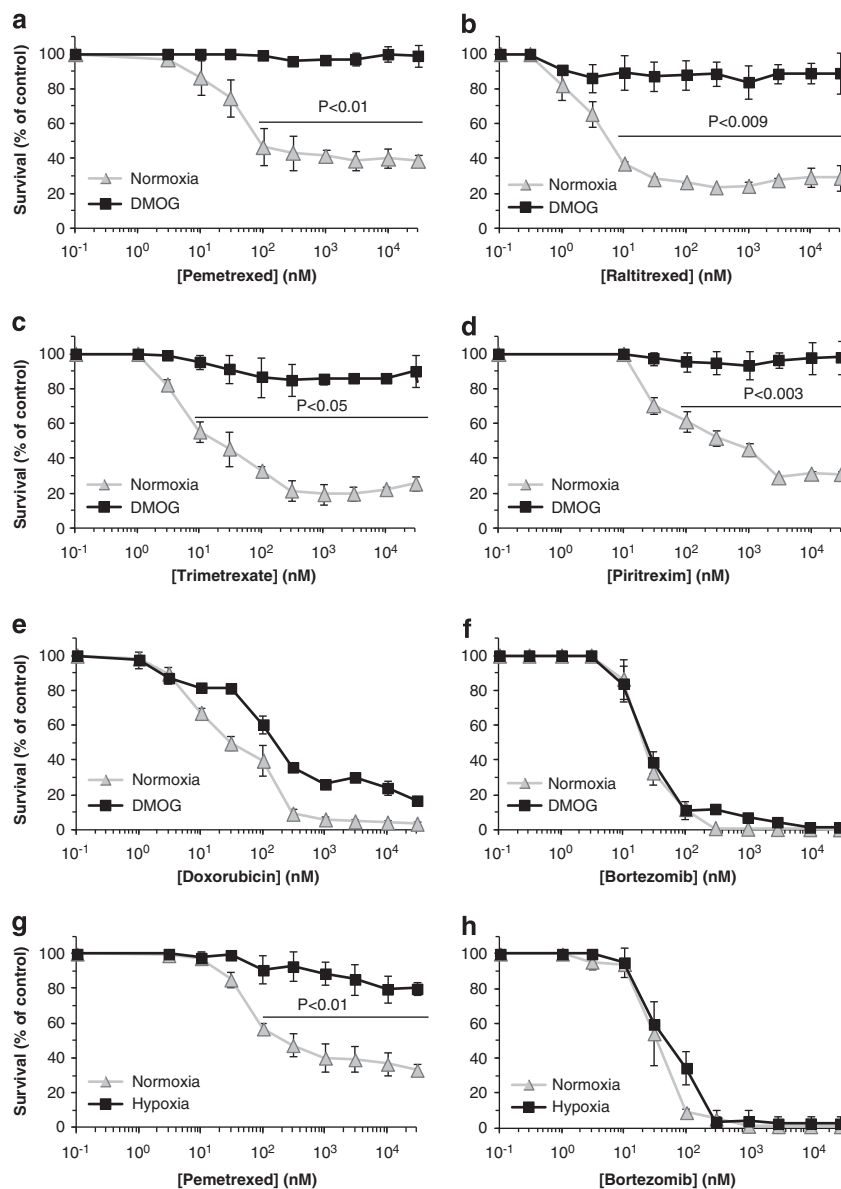
Figure 2 Antifolate growth inhibition assay of HeLa cells under severe hypoxic conditions. Growth inhibition was performed by exposing HeLa cells to increasing concentrations of various cytotoxic drugs with or without 0.5 mM DMOG for 72 h (**a–f**), or severe hypoxia for 24 h (**g** and **h**), and cell survival was determined using the XTT assay. Growth inhibition was assessed using hydrophilic antifolates (**a**, **b** and **g**), lipophilic antifolates (**c** and **d**) or non-antifolate anticancer drugs (**e**, **f** and **h**). Results are normalized to the drug-free control for each treatment and are the means of at least three independent experiments performed in triplicates ± S.D.

4

To further explore antifolate resistance under hypoxia, we determined the sensitivity of HeLa cells to PMX and BTZ under severe hypoxia. HeLa cells were subjected to severe hypoxia ($\leq 0.1\%$ O_2) for 24 h, after which increasing drug concentrations were administered for an additional 24 h under the same conditions. A dramatic PMX resistance was observed under these conditions, at comparable levels to those obtained with DMOG treatment, while retaining sensitivity to BTZ (Figures 2g and h). To expand the scope of our findings, PMX resistance was assessed under DMOG treatment in an assortment of human carcinoma cell lines of different tissue lineage, including HepG2, hepatocellular carcinoma; DLD-1, colorectal adenocarcinoma and MDA-MB, breast carcinoma; tumor cells were co-exposed to 1 μM PMX (10-fold the IC_{50} in HeLa cells) and 0.5 mM DMOG for 72 h, and viable cell numbers were determined using trypan blue exclusion. All tumor cell lines displayed a marked and similar resistance to PMX as observed in HeLa cells (Supplementary Figure S2). There were marked differences between the percentages of viable cells following PMX exposure, as revealed by cell counting (Supplementary Figure S2) and XTT assay (Figure 2a) (5–10 versus 20–40%, respectively), whereas both methods detected 80–100% survival following co-exposure to both PMX and DMOG. As previously shown by Tonkinson et al.,[20] there is a limitation of the XTT assay when combined with antifolates, as cells which survive antifolate treatment respire twice the level of untreated cells, thereby yielding higher XTT values.

Antifolates are known to induce uridine misincorporation leading to mismatch repair with consequent DNA single-strand breaks (SSBs) and double-strand breaks (DSBs),[21] whereas BTZ induces ER stress.[22] To study the basis underlying the marked differences in the cytotoxic activities observed for these drugs under severe hypoxia, we assessed whether or not these cytotoxic drugs can elicit their downstream effects under DMOG treatment. Toward this end, we determined, by western blot analysis, the impact of antifolates on the cellular DNA-damage response (DDR) under conditions of normoxia or hypoxia by monitoring the established DSB[23] and SSB[24] marker histone H2AX S139 phosphorylation, as well as polynucleotide kinase/phosphatase (PNKP) S114 phosphorylation, a DNA DSB marker.[25] We found that 1 μM PMX and TMQ induce high levels of H2AX S139 phosphorylation, most notably after 48 h of treatment, whereas cells exposed to these antifolates under hypoxic conditions were completely devoid of H2AX phosphorylation (Figure 3a). The same results were obtained when monitoring PNKP phosphorylation levels (Supplementary Figure S3).

The expression of BiP/GRP78 was monitored as an established ER-stress marker after BTZ exposure[26] (Figure 3b). In contrast to antifolates, BTZ (80 nM for 24 h) induced high levels of BiP, even under hypoxic conditions (Figure 3b).

Cell cycle arrest is the mechanism underlying antifolate resistance under severe hypoxia. Antifolates induce DNA damage during DNA replication,[1,21] therefore, complete antifolate resistance could be achieved by cell cycle arrest. As hypoxia-induced cell cycle arrest is well documented,[27,28] we postulated that this is the mechanism underlying antifolate resistance, which we observed under severe hypoxic conditions. To corroborate this hypothesis, we first assessed whether our hypoxia system induced cell cycle arrest in HeLa cells. We therefore performed cell cycle analysis using propidium iodide staining following various treatments as detailed in the Materials and Methods section. DNA content was determined under normoxia and compared with severe hypoxic conditions as well as with serum starvation, known to induce cell cycle arrest.[29] Both severe hypoxia and DMOG treatment resulted in a decrease in the percentage of cells in the G_2/M phases and an increase in the percentage of cells in the G_1/S phases (Table 1). Additionally, we used the colorimetric XTT assay to verify that under these conditions cellular proliferation was repressed. Indeed, cells grown under the same conditions divided significantly less; under normoxia, cells divided four times after 96 h, whereas under severe hypoxic conditions cells accomplished up to a single cell doubling (Table 1).
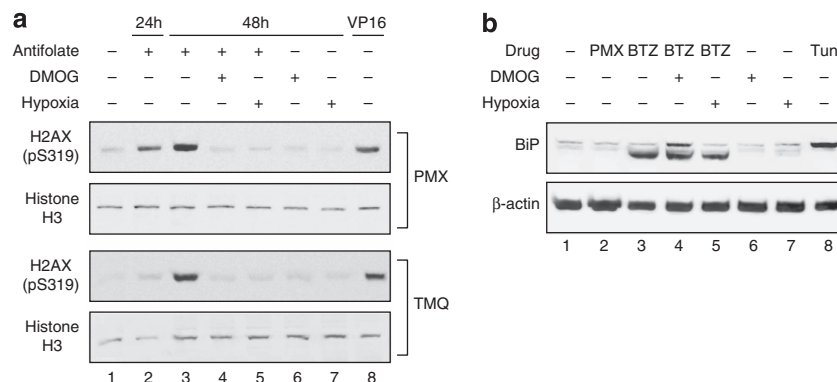

Figure 3 Downstream effects of antifolates and BTZ under DMOG treatment demonstrated by western blot analysis. (**a**) Antifolate-induced H2AX phosphorylation. HeLa cells were exposed to antifolates (i.e., 1 μM PMX or TMQ) under normoxia for 24 or 48 h (lanes 2 and 3), 0.5 mM DMOG for 48 h with or without co-exposure to antifolates (lanes 4 and 6), hypoxia for 48 h with or without co-exposure to antifolates (lanes 5 and 7) and the DNA-damaging agent VP16 (40 μM for 20 min, lane 8). Total protein extracts were subjected to western blotting with a H2AX pS139 antibody. Equal loading was verified by reprobing with a histone H3 antibody. (**b**) BTZ-induced BiP overexpression. HeLa cells were exposed to 1 μM PMX for 24 h (lane 2), 80 nM BTZ under normoxia (lane 3), 0.5 mM DMOG for 24 h with or without co-exposure to 80 nM BTZ (lanes 4 and 6), hypoxia for 24 h with or without co-exposure to 80 nM BTZ (lanes 5 and 7, respectively) and the ER-stress-inducing agent tunicamycin (1 μg/ml for 24 h, lane 8). Cellular proteins were extracted using a hypotonic buffer and subjected to western blotting with a BiP antibody. Equal loading was verified by reprobing with a β-actin antibody

After verifying the induction of cell cycle arrest, we sought to provide evidence that this arrest leads to antifolate resistance. Therefore, the cytotoxic activity of PMX and BTZ in serum-deprived cell cycle-arrested cells was determined. HeLa cells were grown in a medium containing or lacking serum for 24 h, after which the drugs were administered for an additional 72 h under the same conditions. Serum starvation resulted in PMX resistance resembling the dramatic resistance observed under severe hypoxic conditions (compare Figure 4a with Figures 2a and g), whereas cells retained BTZ sensitivity (Figure 4b). In fact, under serum starvation, HeLa cells became > 2-fold more sensitive to BTZ (i.e., $IC_{50} = 7.1 \pm 2.3$ nM and 3.2 ± 0.3 nM in the presence or absence of serum, respectively).

The established viable cell dye carboxyfluorescein diacetate succinimidyl ester (CFSE) was used to monitor cell doublings under normoxia or DMOG treatment, as dilution of intracellular fluorescein occurs after each cell division. The ratio of the CFSE fluorescence under normoxia and DMOG treatment was 9.3 ± 0.7, which correlates with a difference of 3.2 ± 0.1 cell doublings. Moreover, to confirm that cells retain viability under DMOG treatment, thus establishing that the cells are in cell cycle arrest and not in senescence, we performed a recovery experiment. Cells were first exposed to DMOG as indicated in Table 2, after which they were allowed to recover under normoxia for 72 h. For CFSE analysis, cells were labeled before DMOG exposure. The results of this experiment confirmed that the proliferative capacity of the

cells was retained during DMOG exposure, as cells regained cell cycle progression after removal of DMOG, thereby accomplishing three additional cell divisions in 72 h (Supplementary Figure S4). Furthermore, we performed growth inhibition assay with PMX on the recovered cells and confirmed that cells regained PMX sensitivity after exposure to normoxia (Figure 4c).

Discussion

To better understand the poor responsiveness of solid tumors to antifolates, we here investigated the impact of severe hypoxia on carcinoma cells' sensitivity to these antimetabolites. We show here for the first time that severe hypoxia induces complete antifolate resistance due to abrogation of antifolate-induced DNA damage and cell cycle arrest. Our findings indicate that under severe hypoxic conditions (i.e. ≤0.1% oxygen or 0.5 mM DMOG), there is a simultaneous suppression of key genes in folate metabolism genes, including the influx transporters *RFC* and *PCFT*, the efflux transporter *BCRP* as well as the folate-dependent enzymes *DHFR*, *TS*, *GARTF* and *FPGS*. We propose that a common regulatory determinant controls the expression of these genes which is altered under severe hypoxia. It is noteworthy that all the promoters of these genes are TATA-less and GC-rich and are regulated by Sp1[30–37] and most have active CpG islands which were shown to be methylated resulting in gene silencing.[38–42] As it was shown that Sp1 activity can be modulated by hypoxia-induced phosphorylation[43] or by interaction with HIF-1α[44] and that hypoxia results in an increase in DNA-methylation potential,[45] we propose that the collective regulation of folate-metabolism genes could be attributed, at least in part, to alterations in Sp1 activity or promoter methylation of these genes. Apart from serving as methyl donors for purines and thymidylate biosynthesis, reduced folate cofactors are also methyl donors for DNA methylation. Therefore, global promoter methylation of these genes under hypoxia might be explained by folate utilization for DNA methylation on the expense of *de novo* nucleotide biosynthesis. Consistently, we show for the first time that the expression of CNT3 is significantly suppressed under severe hypoxia, in addition to ENT1,2, which were previously reported to be downregulated by HIF-1α,[17,18] suggesting that

Table 1 Cell cycle analysis

	% of cells			Cell divisions[a]
	G_1[b]	S[b]	G_2/M[b]	
Normoxia	47.3 ± 2.3	36.1 ± 4.4	8.4 ± 0.7	4.0 ± 0.5
Hypoxia (≤0.1% O_2)	56.4 ± 4.3	39.6 ± 2.7	2.7 ± 0.6	1.1 ± 0.1
DMOG (0.5 mM)	59.1 ± 8.6	44.1 ± 8	5.1 ± 0.6	0.8 ± 0.1
Serum free	65.5 ± 0.2	27.2 ± 1.5	7.3 ± 1.3	0.2 ± 0.3

Abbreviation: DMOG, dimethyloxalylglycine.
[a]Number of cell divisions during 96 h under the indicated treatment. Numbers presented are the mean of three independent experiments ± S.D.
[b]Cell cycle analysis was performed following 72 h under the indicated treatment. Numbers presented are the means of three independent experiments ± S.D.
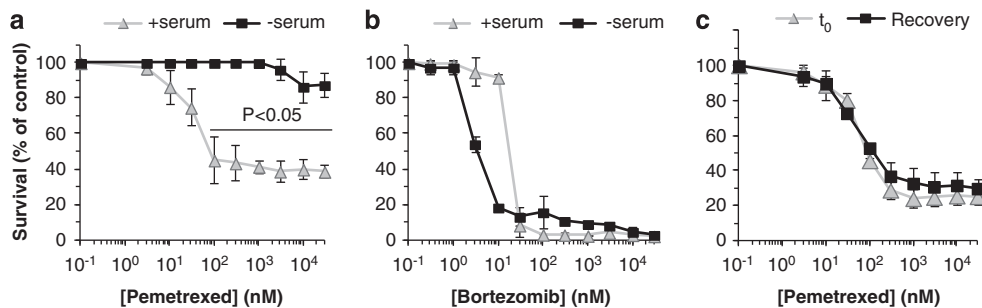

Figure 4 Cell cycle progression determines antifolate resistance and sensitivity. (**a** and **b**) Growth inhibition assay under serum starvation; HeLa cells were grown for 24 h with or without serum, after which increasing drug concentrations were administered for 72 h under the same growth conditions. (**c**) Recovery assay after DMOG treatment; HeLa cells were exposed to DMOG for 88 h (exact details are depicted in Table 2) after which they were allowed to recover for 72 h under normoxia. After recovery, increasing PMX concentrations were administered for 72 h under normoxia. Cell survival was determined using the XTT assay. Results are normalized to the drug-free control for each treatment and are the means of three independent experiments performed in triplicates ± S.D.

Table 2 Experimental conditions for the growth inhibition assay

Treatment	Pre-incubation conditions	Co-incubation conditions
DMOG	16 h, 1 mM DMOG	72 h, 0.5 mM DMOG
Severe hypoxia	24 h, $\leq 0.1\%$ O_2	24 h, $\leq 0.1\%$ O_2
Serum free	24 h, serum-free medium	72 h, serum-free medium

Abbreviation: DMOG, dimethyloxalylglycine

under physiological hypoxic conditions nucleoside uptake is repressed as well.

The second finding here is that carcinoma cells were refractory to antifolates under hypoxic conditions. It has been previously suggested that *DHFR* gene amplification occurs under re-oxygenation of cells following exposure of Chinese hamster ovary cells to hypoxia, resulting in antifolate resistance.[46] However, in our system, human carcinoma cells were refractory to antifolates under severe hypoxic conditions, whereas restoration of normoxia resulted in their resensitization to antifolates. Moreover, cells displayed complete resistance to antifolates that selectively target TS (e.g., raltitrexed and plevitrexed,[1]) or DHFR (i.e., TMQ and PTX). HeLa cell exposure to severe hypoxic conditions resulted in a decreased expression of both *RFC* and *PCFT*, suggesting that the primary transport routes for hydrophilic antifolates are largely inactive. However, altered antifolate transport could not account for the complete resistance to antifolates, as the latter was observed for both hydrophilic and lipophilic antifolates. Moreover, the antifolate exporter *BCRP* was downregulated under severe hypoxic conditions, and whereas the expression levels of *MRP-1* were unchanged, its activity was shown to be markedly decreased under low intracellular folate pools.[47] These alterations should render the tumor cells more sensitive to antifolates,[27] whereas we obtained precisely the opposite here.

Two established mechanisms of drug resistance under hypoxia are the induction of cell cycle arrest and anti-apoptosis.[12] In our current hypoxia system, carcinoma cells retained sensitivity to the non-antifolate drugs BTZ and doxorubicin, while displaying complete resistance to various antifolates. Hence, it is clear that not a general anti-apoptotic effect but rather a more specific mechanism underlies this irresponsiveness to antifolates. Cell cycle analysis as well as CFSE-based cell division assay confirmed that under hypoxic conditions cells are cell cycle arrested. Furthermore, serum starvation, which has been shown to induce cell cycle arrest at the G_1 phase,[29] resulted, on the one hand, in complete antifolate resistance, while inducing BTZ hypersensitivity on the other hand, hence highlighting the key role of cell cycle arrest in antifolate resistance. In this respect, as antifolates induce DNA damage due to uridine misincorporation into the DNA at the S phase,[21] we postulated that as a result of cell cycle arrest, antifolates would not exert DNA damage under hypoxia. Consistently, our findings confirm that under normoxia both PMX and TMQ induce high levels of DNA damage, manifested by histone H2AX and PNKP phosphorylation. This novel finding is the first molecular insight regarding antifolate-induced DDR. Moreover, this effect was abolished under the same hypoxic conditions that promoted cell cycle arrest and

antifolate resistance in HeLa cells. As hypoxic conditions abolished the DDR to both PMX and TMQ, one can conclude that the cellular irresponsiveness to antifolates under hypoxia is independent of their uptake route into the cell.

In contrast to antifolates, BTZ and doxorubicin induce apoptosis in a cell cycle-independent manner; topoisomerase inhibitors were shown to induce DNA damage and apoptosis during all phases of the cell cycle.[23,48] As we have shown here, the proteasome inhibitor BTZ, induced ER stress represented by increased levels of the ER-chaperon BiP/GPR78,[22] even under DMOG treatment. This is supported by recent studies which demonstrated hypersensitivity of human colorectal carcinoma xenografts to BTZ, presumably due to overactivation of the ER stress response under hypoxia.[19]

The suppression of nucleoside biosynthesis has been previously proposed as a mechanism underlying cell cycle arrest under hypoxia. It was specifically shown that exogenous addition of 10–100 μM deoxynucleosides to cells grown under severe hypoxia stimulates progression through the cell cycle.[49,50] However, here we show that the mRNA levels of the NTs are downregulated under severe hypoxia in HeLa cells (except for ENT3, which has the lowest affinity for nucleosides, $K_m \approx 2$ mM). Under DMOG treatment, a small reduction in the expression of ENT1–3 was detected, whereas the expression of CNT3 was reduced by 80%. CNT3 is the only transporter able to translocate all nucleosides with high affinities ($K_m = 15$–43 μM),[16] compatible to the concentrations used in the cell cycle stimulation experiments. Therefore, when we supplemented HeLa cells, under DMOG treatment, with 100 μM (deoxy)nucleosides it failed to restore cell cycle progression. Growth inhibition assay using cytarabine, a nucleoside analog transported by ENT1 and CNT1,3,[16] corroborated this conclusion, as HeLa cells were refractory to cytarabine under DMOG treatment (Supplementary Figure S5).

Based on our current findings along with previous studies, we propose the following composite mechanism for the complete antifolate resistance under hypoxia (Figure 5): 1) Ribonucleotide reductase (RNR), which is responsible for the conversion of ribonucleotides to deoxyribonucleotides, requires oxygen for its catalytic activity and thus is instantaneously inactivated under hypoxia.[51] RNR is the first enzyme in the nucleotide biosynthesis pathway that can respond to hypoxia, hence immediately blocking the last step in deoxynucleotide biosynthesis, resulting in cessation of DNA replication. 2) Under severe hypoxic conditions, HIF1α is stabilized and binds the promoter of the gene encoding the trifunctional enzyme CAD, thus repressing its gene expression[15] (Figure 1c). CAD catalyzes the first three successive reactions in *de novo* pyrimidine biosynthesis, one of which is the rate-limiting step. Hence, CAD controls the rate of DNA synthesis as the most upstream enzyme in the pathway.[52] As *CAD* expression is modulated by HIF1α, CAD acts as a cellular biosensor of oxygen deprivation, which ultimately leads to repression of DNA replication, and cell cycle arrest.[50] Indeed, as evident from Table 1, HeLa cells exposed to DMOG are cell cycle arrested. 3) The third determinant of intracellular nucleotide pool is their uptake. As we have shown, the expression of all NTs is also downregulated under severe hypoxia, abolishing nucleotide pool regeneration. 4) Once cessation of DNA replication occurs, the enzymes
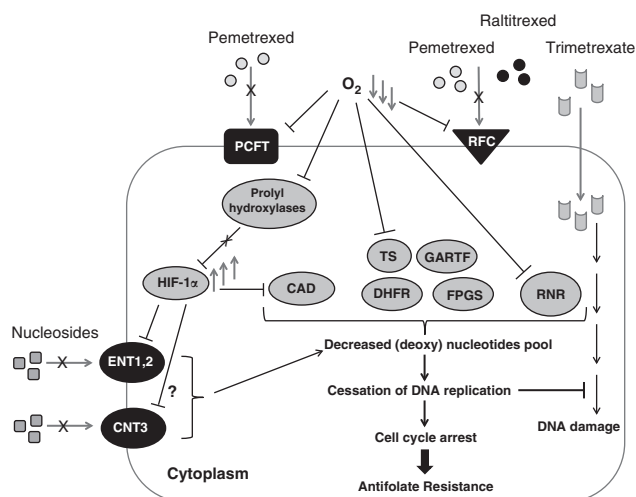
Figure 5 Proposed model of hypoxia-induced cellular processes presumably leading to antifolate resistance. Representation of the cellular proteins in the biosynthesis of nucleotides and folate metabolic pathway that are affected (i.e., silenced or inactivated) by oxygen deprivation. These alterations presumably result in a decreased intracellular pool of (deoxy)nucleotides leading to inhibition of DNA replication and cell cycle arrest. Consequently, these non-dividing cells become refractory to antifolates

in the folate metabolic pathway become dispensable. These enzymes are physiologically crucial for the *de novo* biosynthesis of purines and thymidylate; therefore, they are markedly downregulated. 5) As antifolates exert their cytotoxic activity by inhibiting the key enzymes in the folate metabolic pathway, leading to decreased nucleotide biosynthesis, uridine misincorporation into DNA and DNA damage.[1,21] These antimetabolites become completely useless under severe hypoxia as their normal pharmacologic activity is to inhibit nucleotide biosynthesis, which has already been endogenously suspended.

Materials and Methods

Chemicals. Piritrexim isethionate was a generous gift from Dr. Neil Clendeninn, former Burroughs Wellcome, Research Triangle Park, NC.; Other antifolates were obtained as previously described.[3] Doxorubicin, tunicamycin, cytosine β-D-arabinofuranoside (Cytarabine) and VP16 (etoposide) were from Sigma-Aldrich (St. Louis, MO, USA); Bortezomib (Velcade) was from AdooQ Bioscience (Irvine, CA, USA).

Cell culture. Human HeLa cells (cervical cancer), HepG2 (hepatocellular carcinoma), DLD-1 (colorectal adenocarcinoma) and MDA-MB (breast carcinoma) were maintained as previously described.[30]

Exposure to severe hypoxia and DMOG treatment. To establish hypoxic conditions, cells were placed in a modular incubator chamber (Billups-Rothenberg Inc., Del Mar, CA, USA) that was flushed with $\leq 0.1\%$ O_2, 5% CO_2 and 95% N_2 and incubated at 37 °C. For DMOG (DMOG, Cayman Chemical, Ann Arbor, MI, USA) treatments, DMOG was dissolved in dimethyl sulfoxide and added to the growth medium.

RNA extraction, complementary DNA (cDNA) synthesis and real-time PCR analysis. Cells (10^6) from the mid-log phase of growth were harvested and total RNA was isolated using the TRI Reagent kit (Sigma, St. Louis, MO, USA). RNA was extracted under normoxia or following 18 h in 0.5 mM DMOG or 24 h in severe hypoxia. cDNA synthesis was carried out using the High-Capacity cDNA Reverse Transcription Kit (Applied Biosystems-Life Technologies, Carlsbad, CA, USA).

Gene expression was determined by real-time PCR using an Applied Biosystems-Life Technologies 7300 Real-Time PCR system. Quantitative PCR reaction (20 μl) contained: 5 ng of cDNA, 70 nM of primers and 1 × Power SYBR Green Mix (Applied Biosystems-Life Technologies). The primers used for real-time PCR are depicted in Supplementary Table S1. mRNA expression levels were normalized to β-glucuronidase (*Gus-B*), which was used as an internal control. Each experiment was performed independently at least three times, and all real-time PCR experiments were performed in triplicates.

Growth inhibition assay. Cells were seeded in 96-well plates in growth medium for 24 h. For normoxic and hypoxic conditions, 1000 and 2000 cells were seeded per well, respectively. Cells were then pre-incubated under several conditions (i.e., DMOG, severe hypoxia or serum deprivation), and drugs were added at increasing concentrations. The exact conditions for each treatment are described in Table 2. Untreated cells were simultaneously grown for each treatment for the indicated times and cell survival was determined after 72 h, using a colorimetric cell proliferation kit (XTT, Biological Industries, Kibbutz Beit-Haemek, Israel). Percent survival was calculated relative to drug-free controls. IC_{50} is the drug concentration exerting 50% growth inhibition. Each experiment was performed at least three times in triplicates.

Single-point growth inhibition assay was performed as described in the Supplementary Methods.

For the recovery assay, cells were grown under the same conditions indicated for DMOG treatment in Table 2, after which they were allowed to recover under normoxia for 72 h. Growth inhibition assay was performed again at this time under normoxia as described above.

Western blot analysis. To analyze the levels of early markers of DDR, HeLa cells were exposed to 1 μM PMX or 1 μM TMQ for 24 or 48 h. To assess the impact of hypoxic conditions on antifolate-induced DDR, cells were exposed to 1 mM DMOG or hypoxia ($\leq 0.1\%O_2$) for 16 h, after which the cells were subjected to an additional 48 h under 0.5 mM DMOG or hypoxia in the presence or absence of 1 μM PMX or TMQ. The DNA-damaging topoisomerase II inhibitor VP16 (etoposide, 40 μM for 20 min) served as a positive control. After treatment, proteins were extracted using hot lysis: cells were boiled in lysis buffer (50 mM Tris-HCl pH 8.1, 10 mM EDTA and 1% SDS) at 100 °C for 10 min. The lysates were then sonicated (Misonix Microson, Farmingdale, NY, USA, amplitude 4) twice for 15 s with a 15-s interval.

For ER-stress analysis, HeLa cells were exposed to 1 mM DMOG or hypoxia ($\leq 0.1\%$ O_2) for 16 h, after which cells were subjected to an additional 24 h either under 0.5 mM DMOG or hypoxia with or without 80 nM BTZ, or under 1 μM PMX. The ER-stress inducer tunicamycin (1 μg/ml for 24 h) served as a positive control. Proteins were extracted on ice using a hypotonic buffer (10 mM HEPES pH 7.9, 10 mM KCl, 0.1 mM EDTA, 0.1 mM EGTA, 1 mM DTT, and 0.5% NP-40).

Proteins (40–60 μg) were resolved by electrophoresis on 12.5% or 10% polyacrylamide gels (for DNA damage and ER stress, respectively) containing SDS, electroblotted onto Protran BA83 cellulose nitrate membranes (Schleicher & Schuell, Dassel, Germany), and reacted with the appropriate antibody. Blots were then reacted with a secondary HRP-conjugated antibody (Jackson Immunoresearch Labs, West Grove, PA, USA), and enhanced chemiluminescence (ECL) detection was performed according to the manufacturer's instructions (Biological Industries). ECL was recorded using an LAS-4000 imaging system (Fujifilm Global). Blots were then stripped off and re-probed with a histone H3 (Abcam, Cambridge, MA, USA) or β-actin antibody (Sigma). H2AX p-S139 antibody was from Cell Signaling Technology (Danvers, MA, USA); BiP/GPR78 antibody was from Santa Cruz Biotechnology (Dallas, TX, USA); PNKP p-S114 antibody was kindly provided by Professor Y. Shiloh.

Cell cycle analysis. Cells were exposed to severe hypoxia, 0.5 mM DMOG or serum starvation for 72 h, following which cells were detached by trypsinization (Biological Industries), washed with cold PBS and fixed overnight with ice-cold 70% ethanol. Cells were incubated in PBS containing 40 μg/ml propidium iodide and 100 μg/ml RNase A (Sigma) for 15 min at 37 °C. DNA content was assessed using an LSRII flow cytometer equipped with BD FACSDiVa software version 6.1 and analyzed using the FlowJo v.7.6.5 software.

Calculating the number of cell doublings. The linear relationship between the increase in XTT absorbance and cell numbers was first verified. Then, cells were grown under normoxia and cell numbers were determined after

96 h; this served to determine the number of cell doublings. Calculation of the number of cell divisions under each treatment was performed as follows: the XTT absorbance values in the drug-free control wells from each growth inhibition assay were first measured. The difference in the number of cell doublings under each treatment (i.e., severe hypoxia, DMOG and serum starvation) compared with normoxia was then calculated using the following formula: $A_{norm} = A_{hypo} \times 2^n$, $n = \ln (A_{norm}/A_{hypo})/\ln2$, where A is the absorbance and n is the difference in the number of cell divisions.

Statistical analyses. We used a one-tailed paired Student's t-test to examine the significance of the difference between the control and treatment groups ($N \geq 3$). A difference was considered significant if the P-value obtained was < 0.05.

Conflict of Interest

The authors declare no conflict of interest.

Author contributions

SR, NG, MS, YGA designed the experiments. SR, DS, MS, BB performed the experiments. SR, MS, YGA analyzed the data. SR, MS, YGA prepared the manuscript.

1. Gonen N, Assaraf YG. Antifolates in cancer therapy: structure, activity and mechanisms of drug resistance. *Drug Resist Updat* 2012; **15**: 183–210.
2. Galmarini D, Galmarini CM, Galmarini FC. Cancer chemotherapy: a critical analysis of its 60 years of history. *Crit Rev Oncol Hematol* 2012; **84**: 181–199.
3. Rothem L, Ifergan I, Kaufman Y, Priest DG, Jansen G, Assaraf YG. Resistance to multiple novel antifolates is mediated via defective drug transport resulting from clustered mutations in the reduced folate carrier gene in human leukaemia cell lines. *Biochem J* 2002; **367**(Pt 3): 741–750.
4. Fukumura D, Jain RK. Tumor microenvironment abnormalities: causes, consequences, and strategies to normalize. *J Cell Biochem* 2007; **101**: 937–949.
5. Wang Y, Zhao R, Goldman ID. Characterization of a folate transporter in HeLa cells with a low pH optimum and high affinity for pemetrexed distinct from the reduced folate carrier. *Clin Cancer Res* 2004; **10**(18 Pt 1): 6256–6264.
6. Zhao R, Goldman ID. The molecular identity and characterization of a Proton-coupled Folate Transporter–PCFT; biological ramifications and impact on the activity of pemetrexed. *Cancer Metastasis Rev* 2007; **26**: 129–139.
7. Assaraf YG. Molecular basis of antifolate resistance. *Cancer Metastasis Rev* 2007; **26**: 153–181.
8. Kugel Desmoulin S, Wang L, Hales E, Polin L, White K, Kushner J et al. Therapeutic targeting of a novel 6-substituted pyrrolo [2,3-d]pyrimidine thienoyl antifolate to human solid tumors based on selective uptake by the proton-coupled folate transporter. *Mol Pharmacol* 2011; **80**: 1096–1107.
9. Desmoulin SK, Wang Y, Wu J, Stout M, Hou Z, Fulterer A et al. Targeting the proton-coupled folate transporter for selective delivery of 6-substituted pyrrolo[2,3-d]pyrimidine antifolate inhibitors of de novo purine biosynthesis in the chemotherapy of solid tumors. *Mol Pharmacol* 2010; **78**: 577–587.
10. Gatenby RA, Kessler HB, Rosenblum JS, Coia LR, Moldofsky PJ, Hartz WH et al. Oxygen distribution in squamous cell carcinoma metastases and its relationship to outcome of radiation therapy. *Int J Radiat Oncol Biol Phys* 1988; **14**: 831–838.
11. Wendling P, Manz R, Thews G, Vaupel P. Heterogeneous oxygenation of rectal carcinomas in humans: a critical parameter for preoperative irradiation? *Adv Exp Med Biol* 1984; **180**: 293–300.
12. Shannon AM, Bouchier-Hayes DJ, Condron CM, Toomey D. Tumour hypoxia, chemotherapeutic resistance and hypoxia-related therapies. *Cancer Treat Rev* 2003; **29**: 297–307.
13. Asikainen TM, White CW. HIF stabilizing agents: shotgun or scalpel? *Am J Physiol Lung Cell Mol Physiol* 2007; **293**: L555–L556.
14. Assaraf YG. The role of multidrug resistance efflux transporters in antifolate resistance and folate homeostasis. *Drug Resist Updat* 2006; **9**: 227–246.
15. Chen KF, Lai YY, Sun HS, Tsai SJ. Transcriptional repression of human cad gene by hypoxia inducible factor-1alpha. *Nucleic Acids Res* 2005; **33**: 5190–5198.
16. Molina-Arcas M, Casado FJ, Pastor-Anglada M. Nucleoside transporter proteins. *Curr Vasc Pharmacol* 2009; **7**: 426–434.
17. Morote-Garcia JC, Rosenberger P, Nivillac NM, Coe IR, Eltzschig HK. Hypoxia-inducible factor-dependent repression of equilibrative nucleoside transporter 2 attenuates mucosal inflammation during intestinal hypoxia. *Gastroenterology* 2009; **136**: 607–618.
18. Eltzschig HK, Abdulla P, Hoffman E, Hamilton KE, Daniels D, Schonfeld C et al. HIF-1-dependent repression of equilibrative nucleoside transporter (ENT) in hypoxia. *J Exp Med* 2005; **202**: 1493–1505.
19. Fels DR, Ye J, Segan AT, Kridel SJ, Spiotto M, Olson M et al. Preferential cytotoxicity of bortezomib toward hypoxic tumor cells via overactivation of endoplasmic reticulum stress pathways. *Cancer Res* 2008; **68**: 9323–9330.
20. Tonkinson JL, Marder P, Andis SL, Schultz RM, Gossett LS, Shih C et al. Cell cycle effects of antifolate antimetabolites: implications for cytotoxicity and cytostasis. *Cancer Chemother Pharmacol* 1997; **39**: 521–531.
21. Van Triest B, Pinedo HM, Giaccone G, Peters GJ. Downstream molecular determinants of response to 5-fluorouracil and antifolate thymidylate synthase inhibitors. *Ann Oncol* 2000; **11**: 385–391.
22. Nawrocki ST, Carew JS, Dunner Jr K, Boise LH, Chiao PJ, Huang P et al. Bortezomib inhibits PKR-like endoplasmic reticulum (ER) kinase and induces apoptosis via ER stress in human pancreatic cancer cells. *Cancer Res* 2005; **65**: 11510–11519.
23. Tanaka T, Huang X, Halicka HD, Zhao H, Traganos F, Albino AP et al. Cytometry of ATM activation and histone H2AX phosphorylation to estimate extent of DNA damage induced by exogenous agents. *Cytometry A* 2007; **71**: 648–661.
24. Stiff T, Walker SA, Cerosaletti K, Goodarzi AA, Petermann E, Concannon P et al. ATR-dependent phosphorylation and activation of ATM in response to UV treatment or replication fork stalling. *EMBO J* 2006; **25**: 5775–5782.
25. Segal-Raz H, Mass G, Baranes-Bachar K, Lerenthal Y, Wang SY, Chung YM et al. ATM-mediated phosphorylation of polynucleotide kinase/phosphatase is required for effective DNA double-strand break repair. *EMBO Rep* 2011; **12**: 713–719.
26. Lee AS. The ER chaperone and signaling regulator GRP78/BiP as a monitor of endoplasmic reticulum stress. *Methods* 2005; **35**: 373–381.
27. Goda N, Ryan HE, Khadivi B, McNulty W, Rickert RC, Johnson RS. Hypoxia-inducible factor 1alpha is essential for cell cycle arrest during hypoxia. *Mol Cell Biol* 2003; **23**: 359–369.
28. Kaida A, Miura M. Visualizing the effect of hypoxia on fluorescence kinetics in living HeLa cells using the fluorescent ubiquitination-based cell cycle indicator (Fucci). *Exp Cell Res* 2012; **318**: 288–297.
29. Chen M, Huang J, Yang X, Liu B, Zhang W, Huang L et al. Serum starvation induced cell cycle synchronization facilitates human somatic cells reprogramming. *PLoS One* 2012; **7**: e28203.
30. Stark M, Gonen N, Assaraf YG. Functional elements in the minimal promoter of the human proton-coupled folate transporter. *Biochem Biophys Res Commun* 2009; **388**: 79–85.
31. Bailey-Dell KJ, Hassel B, Doyle LA, Ross DD. Promoter characterization and genomic organization of the human breast cancer resistance protein (ATP-binding cassette transporter G2) gene. *Biochim Biophys Acta* 2001; **1520**: 234–241.
32. Brodsky G, Barnes T, Bleskan J, Becker L, Cox M, Patterson D. The human GARS-AIRS-GART gene encodes two proteins which are differentially expressed during human brain development and temporally overexpressed in cerebellum of individuals with Down syndrome. *Hum Mol Genet* 1997; **6**: 2043–2050.
33. Freemantle SJ, Taylor SM, Krystal G, Moran RG. Upstream organization of and multiple transcripts from the human folylpoly-gamma-glutamate synthetase gene. *J Biol Chem* 1995; **270**: 9579–9584.
34. Horie N, Takeishi K. Functional structure of the promoter region of the human thymidylate synthase gene and nuclear factors that regulate the expression of the gene. *Nucleic Acids Symp Ser* 1995; **34**: 77–78.
35. Park KK, Rue SW, Lee IS, Kim HC, Lee IK, Ahn JD et al. Modulation of Sp1-dependent transcription by a cis-acting E2F element in dhfr promoter. *Biochem Biophys Res Commun* 2003; **306**: 239–243.
36. Whetstine JR, Flatley RM, Matherly LH. The human reduced folate carrier gene is ubiquitously and differentially expressed in normal human tissues: identification of seven non-coding exons and characterization of a novel promoter. *Biochem J* 2002; **367**(Pt 3): 629–640.
37. Zhu Q, Center MS. Evidence that SP1 modulates transcriptional activity of the multidrug resistance-associated protein gene. *DNA Cell Biol* 1996; **15**: 105–111.
38. Wani NA, Hamid A, Kaur J. Alcohol-associated folate disturbances result in altered methylation of folate-regulating genes. *Mol Cell Biochem* 2012; **363**: 157–166.
39. Bram EE, Stark M, Raz S, Assaraf YG. Chemotherapeutic drug-induced ABCG2 promoter demethylation as a novel mechanism of acquired multidrug resistance. *Neoplasia* 2009; **11**: 1359–1370.
40. Enokida H, Shiina H, Igawa M, Ogishima T, Kawakami T, Bassett WW et al. CpG hypermethylation of MDR1 gene contributes to the pathogenesis and progression of human prostate cancer. *Cancer Res* 2004; **64**: 5956–5962.
41. Gonen N, Bram EE, Assaraf YG. PCFT/SLC46A1 promoter methylation and restoration of gene expression in human leukemia cells. *Biochem Biophys Res Commun* 2008; **376**: 787–792.
42. Worm J, Kirkin AF, Dzhandzhugazyan KN, Guldberg P. Methylation-dependent silencing of the reduced folate carrier gene in inherently methotrexate-resistant human breast cancer cells. *J Biol Chem* 2001; **276**: 39990–40000.
43. Lahat N, Bitterman H, Engelmayer-Goren M, Rosenzweig D, Weiss-Cerem L, Rahat MA. Reduced TIMP-2 in hypoxia enhances angiogenesis. *Am J Physiol Cell Physiol* 2011; **300**: C557–C566.
44. Miki N, Ikuta M, Matsui T. Hypoxia-induced activation of the retinoic acid receptor-related orphan receptor alpha4 gene by an interaction between hypoxia-inducible factor-1 and Sp1. *J Biol Chem* 2004; **279**: 15025–15031.

45. Hermes M, von Hippel S, Osswald H, Kloor D. S-adenosylhomocysteine metabolism in different cell lines: effect of hypoxia and cell density. *Cell Physiol Biochem* 2005; **15**: 233–244.

46. Rice GC, Hoy C, Schimke RT. Transient hypoxia enhances the frequency of dihydrofolate reductase gene amplification in Chinese hamster ovary cells. *Proc Natl Acad Sci USA* 1986; **83**: 5978–5982.

47. Hooijberg JH, Jansen G, Assaraf YG, Kathmann I, Pieters R, Laan AC *et al.* Folate concentration dependent transport activity of the Multidrug Resistance Protein 1 (ABCC1). *Biochem Pharmacol* 2004; **67**: 1541–1548.

48. Zhou M, Gu L, Li F, Zhu Y, Woods WG, Findley HW. DNA damage induces a novel p53-survivin signaling pathway regulating cell cycle and apoptosis in acute lymphoblastic leukemia cells. *J Pharmacol Exp Ther* 2002; **303**: 124–131.

49. Loffler M. Restimulation of cell cycle progression by hypoxic tumour cells with deoxynucleosides requires ppm oxygen tension. *Exp Cell Res* 1987; **169**: 255–261.

50. Loffler M. The biosynthetic pathway of pyrimidine (deoxy)nucleotides: a sensor of oxygen tension necessary for maintaining cell proliferation? *Exp Cell Res* 1989; **182**: 673–680.

51. Brischwein K, Engelcke M, Riedinger HJ, Probst H. Role of ribonucleotide reductase and deoxynucleotide pools in the oxygen-dependent control of DNA replication in Ehrlich ascites cells. *Eur J Biochem* 1997; **244**: 286–293.

52. Jones ME. Pyrimidine nucleotide biosynthesis in animals: genes, enzymes, and regulation of UMP biosynthesis. *Annu Rev Biochem* 1980; **49**: 253–279.

Supplementary Information accompanies this paper on Cell Death and Disease website (http://www.nature.com/cddis)